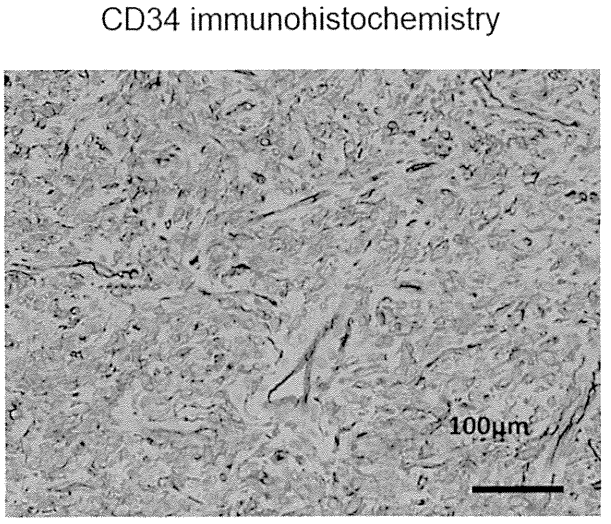

Figure 7. A histologic examination demonstrated a stag-horn vascular pattern and slit-like vascular channels, and CD34 immunohistochemistry detected strong immunoreactivity, which was distinct from the CD34 staining patterns exhibited by solitary fibrous tumors, juvenile angiofibromas, and arteriovenous malformations. Magnification ×100.

juvenile angiofibromas, and AVM (Figure 7). The levator palatine function of the soft palate was maintained, and there was no disruption of swallowing or phonation at 6 postoperative months (Figure 8).

Case 3

A lesion that was diagnosed as an arteriovenous malformation in the parotid gland, but was subsequently found to be an adenoid cystic carcinoma

An 88-year-old male patient had an enlarging mass in his cheek, which had persisted for several years. It had

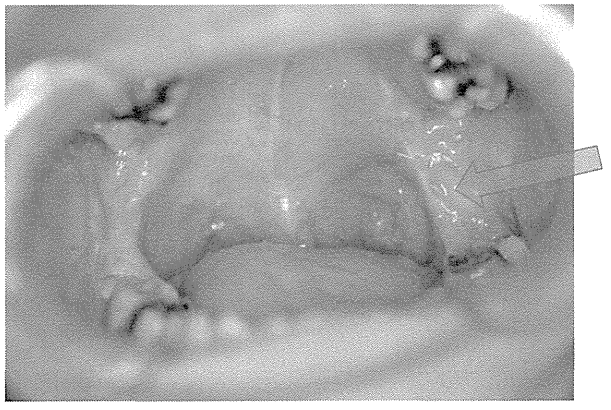

Figure 8. The levator palatine function of the soft palate was maintained, and there was no disruption of swallowing or phonation at 6 postoperative months.

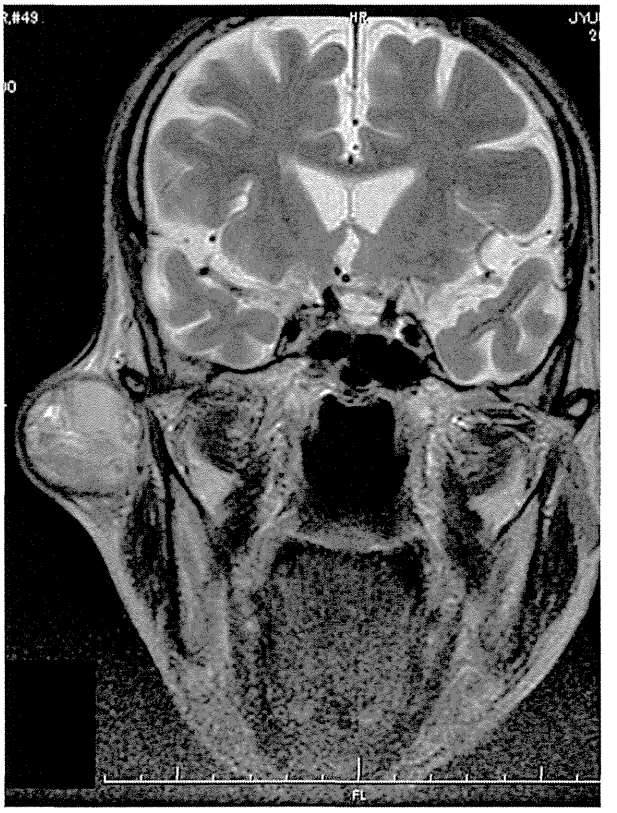

Figure 9. An 88-year-old male patient had noticed an enlarging mass in his cheek, which had been present for several years. The mass measured 5.5 × 5 cm, had a very smooth surface, and was considered to be an atheroma, but marked pulsation had been observed over the last few months. The T2-weighted MRI findings of the lesion were suggestive of a vascular malformation or expanding hematoma.

a very smooth surface, measured 5.5 × 5 cm, and was considered to be an atheroma, but had begun to exhibit marked pulsation over the previous few months. Thus, the patient visited a local clinic, and needle aspiration was performed. Although the latter examination produced a negative result, bloody fluid and blood cells were detected. T2-weighted MRI produced findings that were suggestive of a vascular malformation or an expanding hematoma, but did not detect any invasion into the perineural regions (Figure 9). To regulate the surrounding vasculature, echo-guided transcutaneous sclerotherapy was performed, before the mass was excised, during which no adhesion or invasion into the neighboring tissue was detected. The wound was directly sutured after the resection. Two distinctive types of proliferating cells, ductal cells and myoepithelial cells, were observed during a histologic examination, with the latter being more predominant and exhibiting mild nuclear

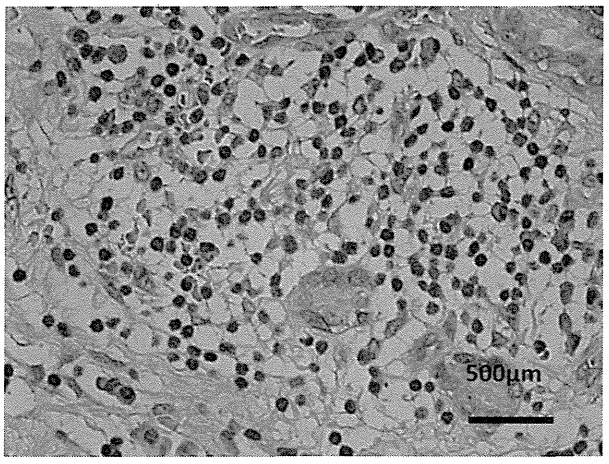

Figure 10. A histologic examination demonstrated 2 distinctive types of proliferating cells, ductal cells and myoepithelial cells, with the latter being more predominant and exhibiting mild nuclear atypia. No invasion into the perineural regions, skin, or exposed surface observed. Adenoid cystic carcinoma was diagnosed. Magnification ×400.

atypia. A myxomatous cribriform pattern within a hyaluronic matrix and a clear tubular pattern were observed. No invasion into the perineural regions, skin, or exposed surface was observed (Figure 10). The mass was found to be an adenoid cystic carcinoma. As the carcinoma was well differentiated and the excision margin was free from tumor cells, further excision was not attempted in accordance with the patient's wishes. Outpatient follow-up ended after 9 postoperative months, and the patient has survived for more than 5 years.

Case 4

A case involving a combination of venous malformation and squamous cell carcinoma in the cheek

A 72-year-old female patient had an erupted vascular malformation on her right cheek, which had been there since childhood. However, superficial skin color changes, growth of the eruption, and alterations in its characteristics over the past few years prompted her to visit a local clinic. A skin biopsy performed at the clinic demonstrated a SCC, which was predominantly composed of small cells with multiple squamous eddies and exhibited a high nuclear/cytoplasmic (N/C) ratio and invasion into the adjacent subcutaneous tissue. The mass, which measured 2 × 1 cm and was located in the right nasolabial fold, was removed by a dermatologist. During the latter procedure, a 1-cm margin from the clinically observable edges of the incision, the scar tissue extending to the masticator muscle fascia, and all adipose tissue were also excised. In addition, echo-guided transcutaneous sclerotherapy was performed to regulate the underlying venous malformation, especially at the edges and the deep parts of the excised region. The buccalis of the facial nerve was partially resected, but no complications were observed during the recovery period, and the venous malformation reduced in size until that it was entirely located within the subcutaneous

TABLE 1. Malignant Tumors That Mimic Vascular Malformations

Malignant Tumor	*Vascular Malformations That the Tumors Mimic*	*Features Resembling Vascular Malformations and Other Information*	*References in This Article*
Malignant peripheral nerve sheath tumor	Coexists with AVF	Common in individuals of 20–50 years of age but can develop earlier in NF-1. Display marked vascularity on imaging	10
Hemangiopericytoma	AVM	Exhibit markedly enhanced blood flow and flow voids	5
Adenocystic carcinoma	AVM	Soft mass, 60% of vascular malformations in the parotid gland occur in the superficial lobe	17
Squamous cell carcinoma	LVM, Klippel–Trenaunay syndrome, AVM	Tend to coexist with massive LVM, can arise from AVM	12,18,19

AVF, arteriovenous fistula; AVM, arteriovenous malformation; LVM, lymphaticovenous malformation; NF-1, neurofibromatosis Type-1.

tissue at 24 postoperative months. Magnetic resonance imaging demonstrated that the area containing the venous malformation partially overlapped with the area from which the SCC had been excised. In contrast, after the resection and sclerotherapy, the T2-weighted signals derived from the venous malformation were less intense in the majority of the subcutaneous tissue and parts of the muscle. Features that can lead to the misdiagnosis of malignant tumors and vascular malformations are listed in Table 1.

Discussion

Malignancies rarely arise from hemangiomas or vascular malformations. In a study of more than 900 pediatric soft tumors, 222 of the cases involved vascular tumors, and capillary hemangiomas were the most common (32%), followed by lymphangiomas (26%). In addition, 4 cases involved malignant lesions; that is, 3 angiosarcomas and 1 case of Kaposi sarcoma, which is almost identical to the findings of our series, although the vascular lesion classifications used in the 2 studies were quite different.[20] In a study of angiosarcomas arising from hemangiomas/vascular malformations, 4 cases involved patients in their sixth or seventh decade of life. These cases initially involved deep masses, and in 3 of the 4 cases, the benign and malignant components were intermixed to varying extents; whereas in the remaining case, the hemangioma/vascular malformation was mainly located at the edge of the malignant tumor. Three cases were associated with AVM, and 1 case was associated with an intramuscular capillary malformation.[21]

Malignant tumors arising from the peripheral nerves are referred to as MPNST, which include malignant schwannoma, neurofibroma, and neurogenic sarcoma.[10] In the above-mentioned case of MPNST (Case 1), preoperative diagnosis based on clinical and imaging examinations suggested a vascular malformation because the mass was located deep in the subcutaneous tissue, was multilobulated, and exhibited high-intensity T2 signals on MRI. In a dynamic study using contrast-enhanced MRI, several venous branches connecting the lesion to the internal mammary veins were observed, and hence, it mimicked a venous malformation. Because venous malformations, unlike other vascular malformations, especially AVM, can exhibit various clinical manifestations, that is, differences in firmness and appearance without bruits or thrills, the diagnosis in cases of suspected venous malformation should be confirmed with US and MRI imaging.[1,2] Magnetic resonance angiography might also be helpful in differentiating between the various types of vascular malformation. Moreover, diffusion-weighted MRI should be used when differentiating malignant tumors from benign tumors or hematomas.[22,23] In contrast, plexiform vascular malformations located near the shoulder might exhibit similar findings to nerve sheath tumors. In a previous study, high-resolution MR neurography and diffusion tensor imaging successfully delineated a slow-flow vascular malformation in a 51-year-old female patient. However, when dynamic contrast MR imaging is not available, large infiltrative lesions can mimic plexiform nerve tumors, and hence, require extensive diagnostic follow-up, including biopsies.[24,25] Although a previous report described a case in which a large hemangiopericytoma was associated with AVM,[5] thrombosis and venous hypertension can result in local increases in angiogenic activity, and pericytes and angiogenesis might play different roles in tumor formation and metastasis.[24] Even if an incorrect preoperative diagnosis is made, interventional radiology, for example, interventional neuroradiologic microvascular bed occlusion with small particles for juvenile angiofibromas, hemangiopericytoma, or AVM, is beneficial for reducing bleeding in subsequent procedures, such as direct sclerotherapy and surgical excision.[25]

In cases involving malignant tumors that appear as well-demarcated mass lesions and display mixed signals on MRI, but are pulsatile, it might not be possible to reach a correct diagnosis. Regarding vascular malformations in the parotid gland, a retrospective study of 614 parotidectomy procedures performed over a 10-year period found that 60% of parotid gland vascular malformations were located in the superficial lobe.[17] In addition, such vascular malformations accounted for 10 (1.6%) of the 614 cases. All 10 cases involved males (mean age, 42 years; range, 19–54 years), and 75% were benign tumors.

Squamous cell carcinoma can arise from ulcers caused by Klippel–Trenaunay syndrome,[18] which is characterized by lymphaticovenous malformations, varicose veins, and hypertrophy of the ipsilateral limb, or from AVM in the scalp.[19] Squamous cell carcinoma tends to occur in chronic ulcerated regions, but it is unclear whether it can also arise from slow-flow vascular malformations. Cases involving malignant tumors and venous malformations without ulceration are not common. However, in a previous case serial ligation, glossectomy was attempted for SCC of the tongue, and the tumor was found to be located adjacent to a massive lymphaticovenous malformation.[12]

Although none of the patients in our series that was treated with absolute ethanol for vascular malformations experienced any negative consequences in terms of tumor management or progression, the possibility of malignancy should be taken into account in cases involving a diagnosis of suspected vascular malformation.

Conclusion

In our series, 4 of 139 vascular malformations exhibited malignancy (a malignant peripheral nerve sheath tumor, a hemangiopericytoma, an adenoid cystic carcinoma, and a SCC); that is, malignancies accounted for 2.88% of suspected vascular malformations. Even when preoperative imaging is performed with US, MRI, CT, and/or angiography and the patient's clinical features and course are taken into account, malignant lesions can be overlooked or misdiagnosed.

References

1. Burrows PE. Endovascular treatment of slow-floe vascular malformations. Tech Vasc Interv Radiol 2013;16:12–21.
2. James CA, Braswell LE, Wright LB, Roberson PK, et al. Preoperative sclerotherapy of facial venous malformations: impact on surgical parameters and long-term follow-up. J Vasc Interv Radiol 2011;22:953–60.
3. Park UJ, Do YS, Park KB, Park HS, et al. Treatment of arteriovenous malformations involving the hands. Ann Vasc Surg 2012;26:643–8.
4. Jeong HS, Baek CH, Son YI, Kim TW, et al. Treatment for extracranial arteriovenous malformations of the head and neck. Acta Otolaryngol 2006;126:295–300.
5. Kalani MY, Martirosyan NL, Eschbacher JM, Nakaji P, et al. Large hemangiopericytoma associated with arteriovenous malformations and dural arteriovenous fistulae. World Neurosurg 2011;76:592.e7–10.
6. Zou X, Liu Q, Zhou X, He G, et al. Ultrasound-guided percutaneous laser and ethanol ablation of rabbit VX2 liver tumors. Acta Radiol 2013;54:181–7.
7. Shin JE, Bark JH, Lee JH. Radiofrequency and ethanol ablation for the treatment of recurrent thyroid cancers: current status and challenges. Curr Opin Oncol 2013;25:14–9.
8. Gritzmann N. Sonography of the salivary glands. AJR Am J Roentgenol 1989;153:161–6.
9. Sigal R, Monnet O, de Baere T, Micheau C, et al. Adenoid cystic carcinoma of the head and neck: evaluation with MR imaging and clinical-pathologic correlation in 27 patients. Radiology 1992;184:95–101.
10. Melloni P, Olsina G, Oliva E, Garcia-Continente G, et al. Atypical inguinal malignant peripheral nerve sheath tumor with arteriovenous fistula of the left femoral nerve in a child. Pediatr Radiol 2008;28:801–56.
11. Nadig M, Munshi I, Short MP, Tonsgard JH, et al. A child with neurofibromatosis-1 and a lumbar epidural arteriovenous malformaton. J Child Neurol 2000;15:273–5.
12. Chien W, Lin HW, Deschler DG. Serial suture ligation glossectomy for squamous cell carcinoma in the settings of a massive lymphovascular malformation. Head Neck 2013;35:E157–60.
13. Akita S, Houbara S, Akatsuka M, Hirano A. Vascular anomalies and wounds. J Tissue Viavility 2013;22:103–11.
14. Al Dhaybi R, Powell J, McCuaig C, Kokta V. Differentiation of vascular tumors from vascular malformations by expression of Wilms tumor 1 gene: evaluation of 126 cases. Journal of the American Academy of Dermatology 2010;63:1052–7.
15. Trindale F, Tellechea O, Torrelo A, Requena L, et al. Wilms tumor 1 expression in vascular neoplasms and vascular malformations. Am J Dermatopathol 2011;33:569–72.
16. Tan WH, Baris HN, Burrows PE, Robson CD, et al. The spectrum of vascular anomalies in patients with PTEN mutations: implications for diagnosis and management. J Med Genet 2007;44:594–602.
17. Achache M, Fakhry N, Varoquaux A, Coulibaly B, et al. Management of vascular malformations of the parotid area. Eur Ann Otorhinolaryngol Head Neck Dis 2013;130:55–60.
18. De Simnone C, Giampetruzzi AR, Guerriero C, De Masi M, et al. Squamous cell carcinoma arising in a venous ulcer as a complication of the Klippel-Trenaunay syndrome. Clin Exp Dermatol 2002;27:209–11.
19. Thomton BP, Sloan D, Rinker B. Squamous cell carcinoma arising from an arteriovenou malformation of the scalp. J Craniofac Surg 2006;17:805–9.
20. Coffin CM, Dehner LP. Vascular tumors in children and adolescents: a clinicopathologic study of 228 tumors in 222 patients. Pathol Annu 1993;28(Pt 1):97–120.
21. Rossi S, Fletcher CD. Angiosarcoma arising in hemangioma/vascular malformation: report of four cases and review of the literature. Am J Surg Pathol 2002;26:1319–29.
22. Einarsdottir H, Karlsson M, Wejde J, Bauer HC. Diffusion-weighed MRI of soft tissue tumors. Eur Radiol 2004;14:959–63.
23. Oka K, Yakushiji T, Sato H, Yorimitsu S, et al. Ability of diffusion-weighed imaging for the differential diagnosis between chronic expanding hematomas and malignant soft tissue tumors. J Magn Reson Imaging 2008;28:1195–200.
24. Raza A, Franklin MJ, Dudek AZ. Pericytes and vessel maturation during tumor angiogenesis and metastasis. Am J Hematol 2010;85:593–8.
25. Turowski B, Zanella FE. Interventional neuroradiology of the head and neck. Neuroimaging Clin N Am 2003;13:619–45.

Address correspondence and reprint requests to: Sadanori Akita, MD, PhD, Department of Plastic and Reconstructive Surgery, Nagasaki University Hospital, 1-7-1 Sakamoto, Nagasaki, 852-8501, Japan, or e-mail: akitas@hf.rim.or.jp

nature COMMUNICATIONS

ARTICLE

Received 16 Dec 2013 | Accepted 27 Jun 2014 | Published 29 Jul 2014

DOI: 10.1038/ncomms5552 OPEN

Myocardium-derived angiopoietin-1 is essential for coronary vein formation in the developing heart

Yoh Arita[1], Yoshikazu Nakaoka[1,2], Taichi Matsunaga[3], Hiroyasu Kidoya[4], Kohei Yamamizu[3], Yuichiro Arima[5], Takahiro Kataoka-Hashimoto[1], Kuniyasu Ikeoka[1], Taku Yasui[1], Takeshi Masaki[1], Kaori Yamamoto[1], Kaori Higuchi[1], Jin-Sung Park[6], Manabu Shirai[7], Koichi Nishiyama[5], Hiroyuki Yamagishi[8], Kinya Otsu[9], Hiroki Kurihara[5], Takashi Minami[10], Keiko Yamauchi-Takihara[1], Gou Y. Koh[6], Naoki Mochizuki[11], Nobuyuki Takakura[4], Yasushi Sakata[1], Jun K. Yamashita[3,12] & Issei Komuro[13,14]

The origin and developmental mechanisms underlying coronary vessels are not fully elucidated. Here we show that myocardium-derived angiopoietin-1 (Ang1) is essential for coronary vein formation in the developing heart. Cardiomyocyte-specific *Ang1* deletion results in defective formation of the subepicardial coronary veins, but had no significant effect on the formation of intramyocardial coronary arteries. The endothelial cells (ECs) of the sinus venosus (SV) are heterogeneous population, composed of APJ-positive and APJ-negative ECs. Among these, the APJ-negative ECs migrate from the SV into the atrial and ventricular myocardium in Ang1-dependent manner. In addition, Ang1 may positively regulate venous differentiation of the subepicardial APJ-negative ECs in the heart. Consistently, *in vitro* experiments show that Ang1 indeed promotes venous differentiation of the immature ECs. Collectively, our results indicate that myocardial Ang1 positively regulates coronary vein formation presumably by promoting the proliferation, migration and differentiation of immature ECs derived from the SV.

[1] Department of Cardiovascular Medicine, Osaka University Graduate School of Medicine, 2-2, Yamadaoka, Suita, Osaka 565-0871, Japan. [2] Precursory Research for Embryonic Science and Technology (PRESTO), Japan Science Technology Agency, 4-1-8, Honcho, Kawaguchi, Saitama 332-0012, Japan. [3] Laboratory of Stem Cell Differentiation, Institute for Frontier Medical Sciences/Department of Cell Growth & Differentiation, Center for iPS Cell Research and Application (CiRA), Kyoto University, 53, Shogoin-Kawahara-cho, Sakyo-ku, Kyoto 606-8507, Japan. [4] Department of Signal Transduction, Research Institute for Microbial Diseases, Osaka University, 3-1, Yamadaoka, Suita, Osaka 565-0871, Japan. [5] Department of Physiological Chemistry and Metabolism, Graduate School of Medicine, University of Tokyo, 7-3-1, Hongo, Bunkyo-ku, Tokyo 113-0033, Japan. [6] National Research Laboratory of Vascular Biology and Stem Cells, Graduate School of Medical Science and Engineering, Korea Advanced Institute of Science and Technology (KAIST), 373-1, Guseong-dong, Daejeon 305-701, Korea. [7] Department of Bioscience, National Cerebral and Cardiovascular Center Research Institute, 5-7-1, Fujishirodai, Suita, Osaka 565-8565, Japan. [8] Department of Pediatrics, Keio University School of Medicine, 35, Shinano-machi, Shinjuku-ku, Tokyo 160-8582, Japan. [9] Cardiovascular Division, King's College London, 25, Coldharbour Lane, London SE5 9NU, UK. [10] Laboratory for Vascular Biology, Research Center for Advanced Science and Technology, University of Tokyo, 4-6-4, Komaba, Meguro-ku 153-8904, Tokyo, Japan. [11] Department of Cell Biology, JST-CREST, National Cerebral and Cardiovascular Center Research Institute, 5-7-1, Fujishirodai, Suita, Osaka 565-8565, Japan. [12] Department of Stem Cell Differentiation, Institute for Frontier Medical Sciences, Kyoto University, 53, Shogoin-Kawahara-cho, Sakyo-ku, Kyoto 606-8507, Japan. [13] Department of Cardiovascular Medicine, Graduate School of Medicine, University of Tokyo, 7-3-1, Hongo, Bunkyo-ku, Tokyo 113-0033, Japan. [14] Core Research for Evolutional Science and Technology (CREST), Japan Science Technology Agency, 4-1-8, Honcho, Kawaguchi, Saitama 332-0012, Japan. Correspondence and requests for materials should be addressed to Y.N. (email: ynakaoka@cardiology.med.osaka-u.ac.jp).

As the heart develops and the chamber walls thicken during embryonic development, passive diffusion of oxygen and nutrients is replaced by a vascular plexus, which is remodelled and expands to form a mature coronary vascular system[1,2]. The coronary arteries and veins ensure the continued development of the heart and progressively increase cardiac output towards birth. Elucidating the cellular and molecular signals involved in vascularizing the embryonic heart would provide significant insights into adult heart disease and tissue regeneration. However, many aspects of the developmental origins of coronary endothelial cells (ECs) and the specific signals determining their fate have not been fully elucidated to date[2,3].

The heart is arranged in three layers: the endocardium, myocardium and epicardium. The epicardium is the outermost layer and is derived from the proepicardium located outside, but close to the heart. The myocardium is the central layer, within which the coronary vasculature develops. It is unclear whether proepicardium/epicardial cells contribute significantly to coronary EC formation in mammals, although some coronary ECs in avian species are derived from proepicardial cells[4–6]. However, more recent studies in mammals demonstrated that epicardial cells generate coronary vascular smooth muscle cells but not coronary ECs[7,8]. A recent report showed that the coronary vessels in mammals are primarily derived from a common origin, the differentiated venous ECs in the sinus venosus (SV), a major vein located just above the developing liver that returns blood to the embryonic heart[9]. According to that report, the sprouting venous ECs dedifferentiate when they migrate over or invade the myocardium. The intramyocardial invading ECs redifferentiate into arteries, whereas the ECs proceeding along the subepicardial layer of the heart redifferentiate into veins[9]. Another recent study reported that the Semaphorin3D/Scleraxis lineage-traced proepicardial cells, which traverse through SV endothelium en route to the heart and/or transiently contribute to the endocardium, differentiate into the coronary ECs[10]. A more recent report suggested that endocardial ECs generate the endothelium of coronary arteries through myocardial–endothelial signalling by vascular endothelial growth factor-A (VEGF-A) and vascular endothelial growth factor receptor 2 (VEGFR2)[11]. These findings suggest that coronary arteries and veins have distinct origins and are formed by different molecular mechanisms. Especially, the molecular mechanisms of coronary vein formation have been elusive to date.

Angiopoietin-1 (Angl) is a member of the angiopoietin family of growth factors and is a major ligand for Tie2, a tyrosine kinase receptor primarily expressed on ECs[12,13]. Angl/Tie2 signalling is required for EC quiescence, pericyte recruitment and the formation of stable vessels[12]. The Angl/Tie2 signalling pathway is critical for normal development, since conventional *Angl* or *Tie2* knockout mice exhibit embryonic lethality between E9.5 and E12.5, with similar abnormal vascular phenotypes and loss of heart trabeculation[14,15]. We previously found that neuregulin-1(NRG-1)/ErbB signalling is essential for cardiac homeostasis presumably via Angl secreted from cardiomyocytes[16]. Thus, we investigated the role of myocardial-derived Angl in coronary vessel formation and cardiac homeostasis by creating cardiomyocyte-specific Angl-knockout mice.

In the present study, we show that myocardium-derived Angl is indispensable for coronary vein formation in the developing heart. Cardiomyocyte-specific *Angl* deletion results in defective formation of the subepicardial coronary veins, but does not affect the formation of the intramyocardial coronary arteries. The ECs of the SV consist of two heterogeneous populations, namely APJ-positive and APJ-negative ECs. Among these, the APJ-negative ECs migrate from the SV into the atrial and ventricular myocardium in Angl-dependent fashion. In addition, Angl promotes venous differentiation of the subepicardial APJ-negative ECs in the heart. Furthermore, *in vitro* experiments using the Flk1-positive immature endothelial progenitor cells demonstrate that Angl indeed promotes venous differentiation. Taken together, these findings suggest that myocardial Angl has an essential role in coronary vein formation presumably by promoting the proliferation, migration and differentiation of immature ECs derived from the SV.

Results

Myocardial deletion of *Angl* results in embryonic lethality. We hypothesized that myocardium-derived Angl is essential for heart development by mediating coronary vessel formation. To test this hypothesis, we generated cardiomyocyte-specific *Angl*-knockout (Angl CKO) mice using the *Cre-loxP* system. We created an $Angl^{flox}$ allele by introducing two *loxP* sites into introns flanking exon 1, which encodes part of the signal sequence[17]. To generate Angl CKO mice, we crossed $Angl^{flox/flox}$ mice with *α-MHC-Cre* transgenic mice[16]. We confirmed the expected genetic recombination at the *Angl* locus in the heart, but not in the head of Angl CKO ($Angl^{flox/flox}$; *α-MHC-Cre*) embryos (Supplementary Fig. 1a). We also confirmed that *Angl* mRNA was ablated from the ventricles of Angl CKO embryos compared with that of control ($Angl^{flox/flox}$) embryos by whole-mount *in situ* hybridization (Supplementary Fig. 1b)[18]. In addition, *Angl* mRNA expression was significantly reduced in the hearts of Angl CKO embryos compared with those of control embryos at E8.5-E10.5 as assessed by quantitative reverse transcription –PCR (qRT–PCR; Supplementary Fig. 1c). Consistently, we confirmed that the Cre-mediated recombination at E8.5 and E9.5 through crossing *α-MHC-Cre* mice with enhanced GFP reporter mice (*CAG-CAT-EGFP* mice) (Supplementary Fig. 1d). No live Angl CKO mice were obtained, and Angl CKO embryos died in uterus between E12.5 and E14.5, slightly later than conventional Angl-knockout (Angl KO) mice, which die at E12.5 (Supplementary Table 1)[15,19].

Angl CKO embryos show defects in coronary vein formation. To examine the effect of myocardial deletion of Angl on the coronary vessel formation, we performed a histological analysis of the hearts of Angl CKO embryos. Whole-mount CD31-immunostaining revealed that Angl CKO embryos exhibited impaired subepicardial coronary vessel remodelling compared with control embryos (Fig. 1a–d, Supplementary Fig. 2a–d). The whole-mount stained samples were then sectioned for analysis. The subepicardial CD31-positive vessel formation was specifically disturbed in Angl CKO embryos (Fig. 1e,f), whereas the intramyocardial CD31-positive vessel formation was almost similar in control and Angl CKO embryos (Fig. 1e,f,h). Although the subepicardial CD31-positive vessels were detected uniformly from the dorsal to ventral side in the ventricles of control embryos (Fig. 1e), the number of subepicardial CD31-positive vessels gradually decreased from the dorsal (Fig. 1f, area 1) to ventral side (Fig. 1f, area 3) in the ventricles of Angl CKO embryos. The number of subepicardial CD31-positive coronary vessels in the transverse section containing the inflow-tract area in Angl CKO embryos was indeed smaller by 57% than that of control (Fig. 1g), indicating that the cardiomyocyte-specific deletion of *Angl* resulted in the impaired formation of subepicardial CD31-positive coronary vessels in the heart.

The subepicardial and intramyocardial CD31-positive vessels are reported to give rise to the coronary veins and arteries, respectively[9,20]. Thus, our findings suggest that the cardiomyocyte-specific deletion of *Angl* may lead to defective

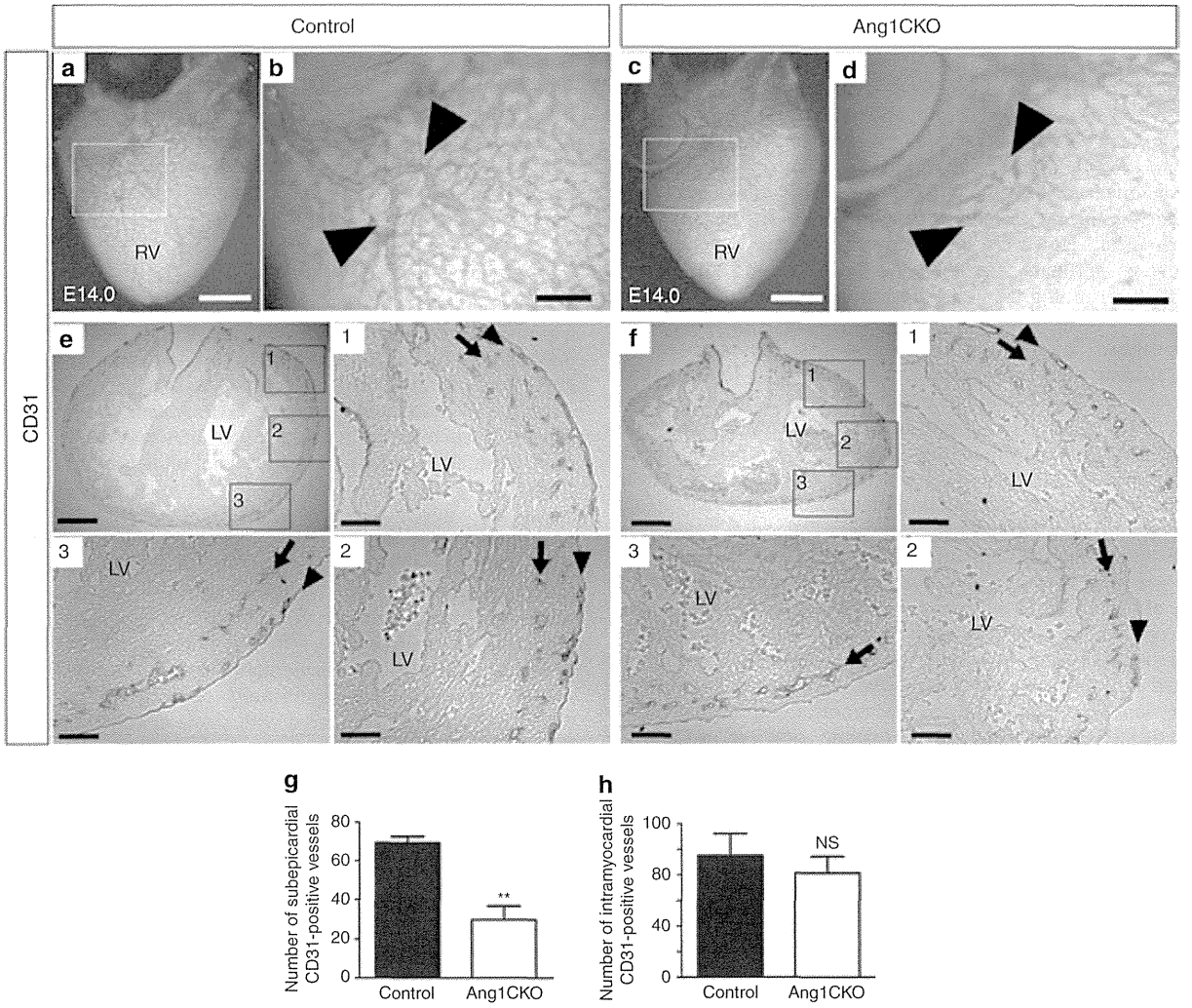

Figure 1 | Myocardial Ang1 is crucial for subepicardial coronary vessel formation. (**a**–**d**) Whole-mount immunostaining of embryonic hearts at E14.0 with anti-CD31 antibody. Myocardial Ang1 was required for subepicardial CD31-positive vessel remodelling (**a**,**b**: arrowheads in magnified image of inset). The CD31-positive vessel formation was impaired in the ventricles of Ang1CKO embryos (**c**,**d**: arrowheads in magnified image of inset). (**e**,**f**) Sectioned analysis of the whole-mount immunostained embryonic heart. Subepicardial CD31-positive vessels were detected uniformly in all the sections from control embryo ventricles (**e**), whereas the density of subepicardial CD31-positive vessels decreased gradually from the dorsal (area 1) to the ventral side (area 3) in Ang1CKO embryos (**f**). Arrows and arrowheads indicate the intramyocardial CD31-positive vessels and subepicardial CD31-positive vessels, respectively. Area 1, dorsal side; area 2, lateral side; area 3, ventral side of the ventricles. (**g**,**h**) Quantification of the number of subepicardial and intramyocardial CD31-positive vessels in the transverse section including inflow-tract of ventricle from E14.0 ($n=3$). Scale bars, 400 μm in **a**,**c**; 100 μm in **b**,**d**; 200 μm in **e**,**f**; and 50 μm in magnified images of insets 1–3. LV, left ventricle; RV, right ventricle. Values are shown as means ± s.e.m. for three separate experiments. Student's *t*-test was used to analyse differences. $^{**}P<0.01$ compared with control. NS, not significant.

formation of the subepicardial coronary veins. To characterize the lost vessels in the hearts of Ang1CKO embryos, we examined the expression of APJ, which is confined to the veins, by whole-mount immunostaining[21,22]. Intriguingly, APJ-positive subepicardial venous vessels were observed in both atria and ventricles of control embryos, but not in those of Ang1CKO embryos (Fig. 2a–d, Supplementary Fig. 3a,b). Analysis of the sectioned samples clearly revealed subepicardial APJ-positive vessel structures in the control but not in the Ang1CKO embryos (Fig. 2e–h, Supplementary Fig. 3c,d), suggesting that cardiomyocyte-derived Ang1 is required for the formation of subepicardial APJ-positive mature coronary veins.

To examine the expression of Eph receptor B4 (EphB4), another venous endothelial marker, in the Ang1CKO embryos, we created *Ang1flox/flox; α-MHC-Cre(+); EphB4 tau-lacZ(+)* by crossing *Ang1+/flox; α-MHC-Cre*-TG mice with *EphB4 tau-lacZ* knockin mice, which express the *lacZ* reporter gene in the venous ECs[23]. EphB4-lacZ-positive signals were observed in the subepicardial region of the hearts of control embryos at E13.0, but not in those of Ang1CKO embryos (Fig. 2i–l, Supplementary Fig. 3e–h).

Chicken ovalbumin upstream promoter-transcription factor II (COUP-TFII), is reported to be a critical transcription factor for the venous identity of ECs[24,25]. *In situ* hybridization revealed that the expression of *COUP-TFII* is observed in the subepicardial region of the hearts of control embryos at E13.5, but not in those of Ang1CKO embryos (Fig. 2m–p). The numbers of subepicardial differentiated coronary veins identified by APJ-positive vessels, EphB4-lacZ-positive vessels and *COUP-TFII*-positive vessels in Ang1CKO embryos were

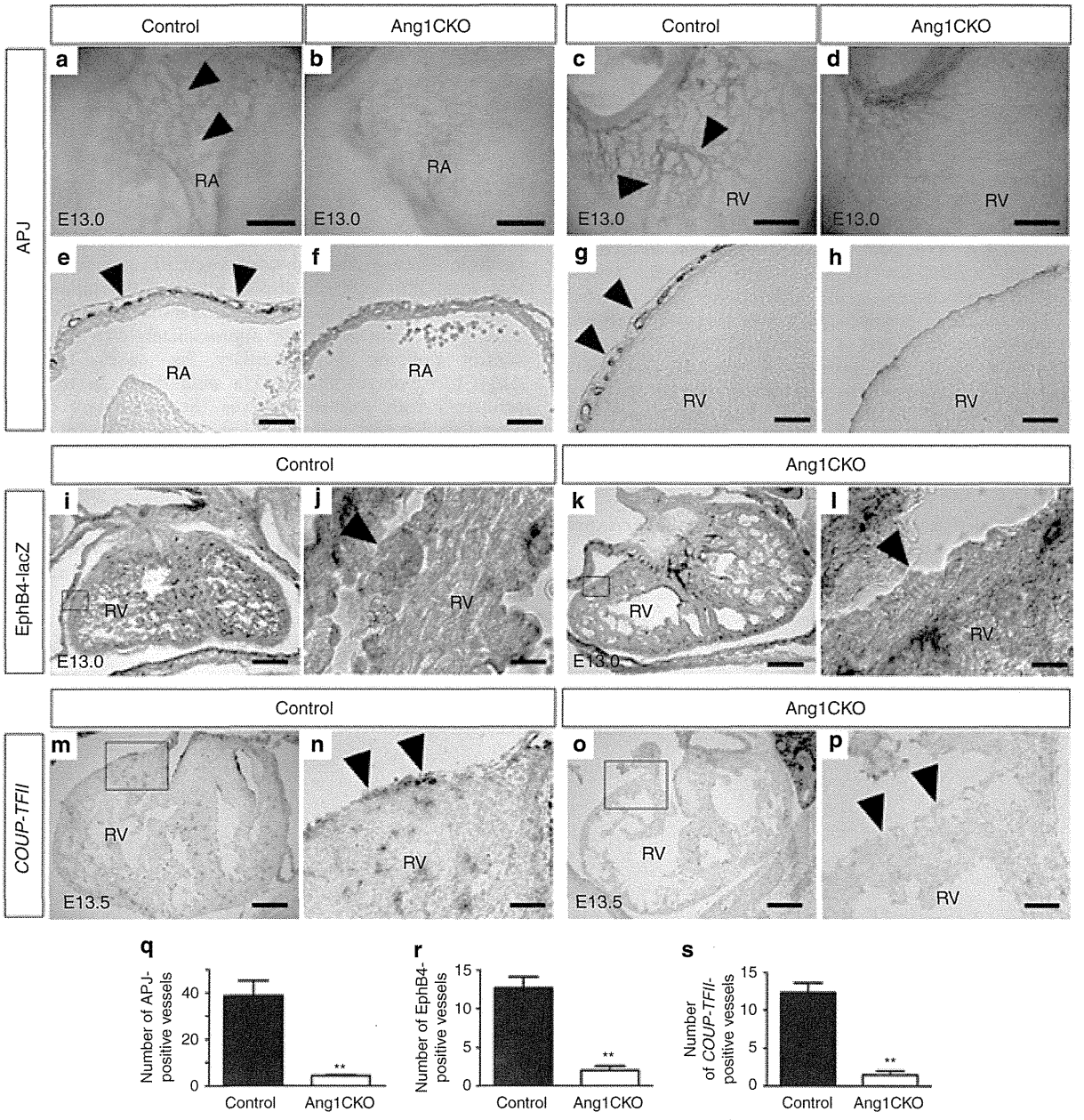

Figure 2 | Myocardial Ang1 is essential for coronary vein formation. (**a**–**d**) Whole-mount immunostaining of embryonic hearts with anti-APJ antibody. APJ-positive coronary veins were observed on the surfaces of both the RA (**a**, arrowheads) and RV (**c**, arrowheads) of control embryos, but not on the RA (**b**) or RV (**d**) of Ang1CKO embryos. (**e**–**h**) Sectioned analyses of the whole-mount immunostained embryonic hearts revealed subepicardial APJ-positive coronary veins with vessel-like structures in the RA (**e**, arrowheads) and RV (**g**, arrowheads) of control, but not Ang1CKO embryos (**f**,**h**). (**i**–**l**; Note: for the experiment presented in **i**–**l**, both 'control' and 'Ang1CKO' mice contained the *EphB4 tau-lacZ* knockin allele; see Results.) EphB4-lacZ-positive signals in the hearts of control and Ang1CKO embryos at E13.0. EphB4-lacZ-positive subepicardial coronary veins were observed in control (**i**,**j**, arrowhead), but not Ang1CKO embryos (**k**,**l**, arrowhead). EphB4-lacZ-positive signals were also detected in the endocardial endothelium in both control and Ang1CKO embryos. (**m**–**p**) Expression patterns of *COUP-TFII* in the hearts at E13.5. *COUP-TFII*-positive subepicardial coronary veins were observed in control (**m**,**n**, arrowhead), but not in Ang1CKO embryos (**o**,**p**, arrowhead). (**q**–**s**) Quantification of the number of subepicardial APJ (**q**, E13.5), EphB4-lacZ (**r**, E13.0) and *COUP-TFII* (**s**, E13.5) -positive vessels in the transverse section including inflow-tract of ventricle ($n=3$). (**r**) The number of the EphB4-positive vessels especially with vessel-like structures or with red blood cells were quantified. Scale bars, 100 μm in **a**–**h**; 300 μm in **i**,**k**,**m**,**o**; 25 μm in **j**,**l**; and 75 μm in **n**,**p**. RA, right atrium; RV, right ventricle. Values are shown as means ± s.e.m. for three separate experiments. Student's *t*-test was used to analyse differences. $^{**}P<0.01$ compared with control.

reduced by 84–89% compared with those of control embryos (Fig. 2q–s). In addition, the quantification revealed that the number of subepicardial mature coronary veins positive for the above venous markers in the ventricles was much less than that of subepicardial immature CD31-positive vessels. Taken together, these findings suggest that cardiomyocyte-specific deletion of *Ang1* impairs the formation of subepicardial coronary veins.

Ang1CKO embryos show no defects in coronary artery formation. Next, we examined the effect of cardiomyocyte-specific *Ang1* deletion on the formation of coronary arteries. Since the coronary arteries penetrate the aorta at E13.5 (ref. 1), we performed coronary angiography in E13.5 embryos using an ink injection technique (see Methods)[26]. The results revealed that there was no significant difference in coronary artery formation between the control and Ang1CKO embryos (Fig. 3a–d).

To confirm the expression of arterial endothelial marker EphrinB2 in the Ang1CKO embryos, we created *Ang1flox/flox; α-MHC-Cre(+); EphrinB2 tau-lacZ(+)* mice by crossing *Ang1+/flox; α-MHC-Cre*-TG mice with *EphrinB2 tau-lacZ* knockin mice, which express the *lacZ* reporter gene in arterial ECs[27]. EphrinB2-lacZ-positive signals were comparably observed in the intramyocardial layers of control and Ang1CKO embryos at E13.0 (Fig. 3e–h). The number of EphrinB2-lacZ-positive vessels in Ang1CKO embryos was almost similar to that in control embryos (Fig. 3i). These findings suggest that cardiomyocyte-specific deletion of *Ang1* did not affect the formation of the intramyocardial coronary arteries.

Myocardial deletion of *Ang1* reduces venous marker expression. To confirm the defect in coronary vein formation in Ang1CKO embryos quantitatively, we examined the expression levels of venous marker genes including *APJ, Ephb4* and *COUP-TFII*[28]. The expression levels of these mRNAs were significantly reduced in the hearts of Ang1CKO embryos compared with those of controls (Fig. 4a–c). In contrast, the expression levels of arterial marker genes such as *Efnb2, neuropilin-1 (Nrp1), Delta-like 4 (Dll4), hairy and enhancer of split 1 (Hes1), activin receptor-like kinase 1 (Acvrl1)* and *Notch1* were not significantly affected in the hearts of Ang1CKO embryos compared with those of controls (Fig. 4d–i). These data indicate that myocardial Ang1 is specifically involved in the formation of coronary veins, but not coronary arteries.

Ang1CKO embryos display impaired development of myocardium. Through the analysis of Ang1CKO embryos, we noticed that Ang1CKO embryos display impaired development of the hearts. The thicknesses of compact layers in Ang1CKO embryos were significantly thinner by approximately 40% than those in control embryos (Supplementary Fig. 4a–d). In addition, Ang1CKO embryos displayed a mild defect in trabeculation compared with control embryos (Supplementary Fig. 4a,b). Therefore, we next performed immunostaining with anti-phospho-histone H3 (pHH3) antibody. Ang1CKO embryos display impaired proliferation of cardiomyocytes compared with control embryos (Supplementary Fig. 4e–g). We previously reported that NRG-1/ErbB signalling is essential for cardiac homeostasis presumably in part via secretion of Ang1 from cardiomyocytes[16]. NRG-1 is an EGF-family growth factor, which is essential for myocardial growth and trabeculation through the activation of ErbB receptors during embryogenesis[29]. Thus, we examined whether myocardial deletion of Ang1 might affect the expression

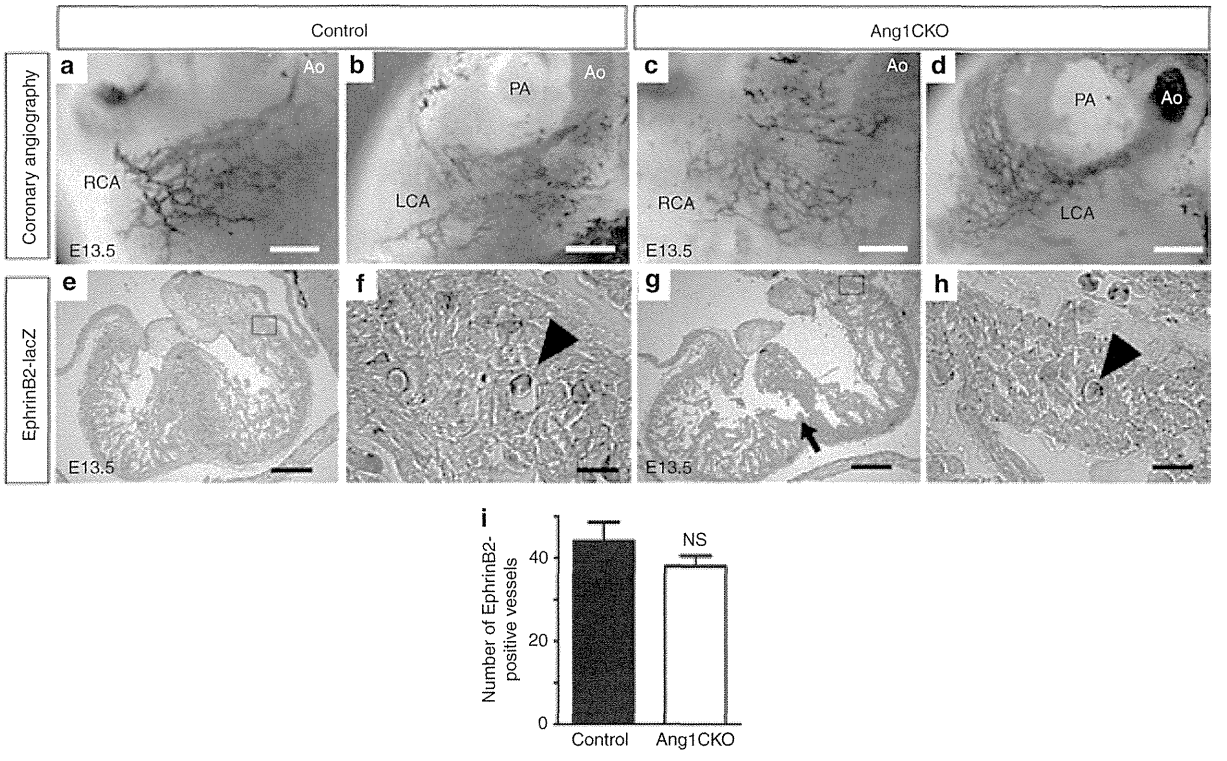

Figure 3 | Myocardial Ang1 is dispensable for coronary artery formation. (**a–d**) Coronary angiography by ink injection into the hearts of control (**a**,**b**) and Ang1CKO embryos (**c**,**d**) at E13.5. (**e–h**; Note: for the experiment presented in **e–h**, both 'control' and 'Ang1CKO' mice contained the *EphrinB2 tau-lacZ* knockin allele; see Results.) EphrinB2-lacZ-positive signals in the hearts of control and Ang1CKO embryos at E13.5. EphrinB2-lacZ-positive intramyocardial coronary arteries (containing red blood cells) were similarly observed in control (**e**,**f**, arrowhead) and Ang1CKO embryos (**g**,**h**, arrowhead). The arrow indicates impaired formation of the interventricular septum in Ang1CKO embryos. (**i**) Quantification of the number of RV + LV free wall EphrinB2-lacZ-positive vessels in the transverse section including inflow-tract of ventricle from E13.5 ($n = 3$). Scale bars, 100 μm in **a–d**; 300 μm in **e**,**g**; and 50 μm in **f**,**h**. Ao, aorta; LCA, left coronary artery; RCA, right coronary artery. Values are shown as means ± s.e.m. for three separate experiments. Student's *t*-test was used to analyse differences. NS, not significant.

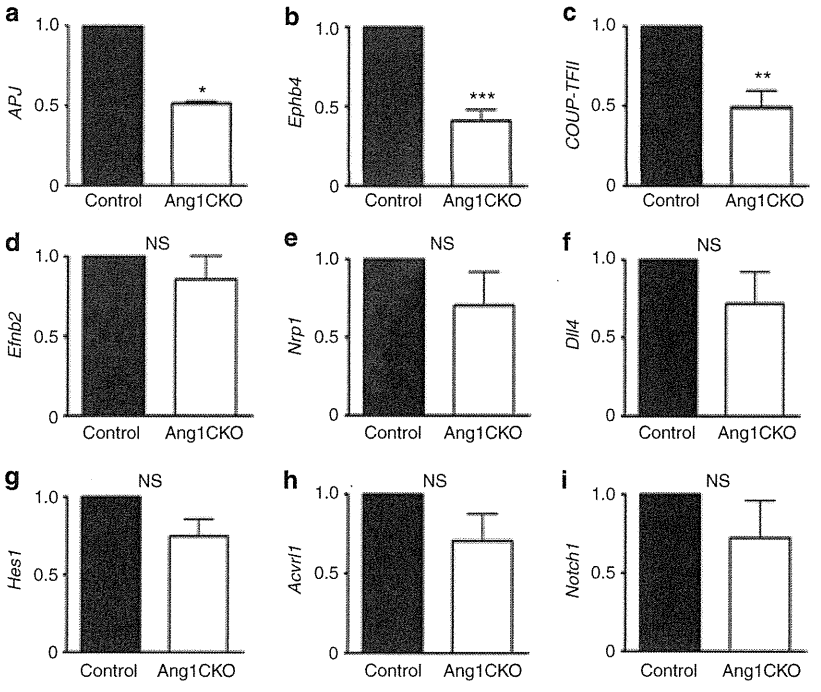

Figure 4 | The expression levels of venous marker genes are significantly lower in the hearts of Ang1CKO embryos than in those of control. (**a–i**) Quantitative expression analysis of venous and arterial marker mRNAs in the ventricles at E12.5-E13.0 (normalized to *GAPDH* mRNA; $n=3$). The expression levels of venous marker genes such as *APJ* (**a**), *Ephb4* (**b**), *COUP-TFII* (**c**), were significantly reduced in Ang1CKO embryos compared with control. However, the expression levels of arterial marker genes such as *EfnbB2* (**d**), *Nrp1* (**e**), *Dll4* (f), *Hes1* (**g**), *Acvrl1* (**h**) and *Notch1* (**i**) were not significantly affected in Ang1CKO embryos compared with control. Values are shown as means ± s.e.m. for three separate experiments. Student's *t*-test was used to analyse differences. $^{*}P<0.05$, $^{**}P<0.01$, $^{***}P<0.001$ compared with control. NS, not significant.

level of NRG-1 in the hearts. We found that the mRNA level of *Nrg-1* in the hearts of Ang1CKO embryos was significantly lower than in those of control embryos (Supplementary Fig. 4h). Therefore, the reduced myocardial growth of Ang1CKO embryos might be partly attributed to the reduced expression of *Nrg-1* gene in the hearts of Ang1CKO embryos. In addition, we also found that the formation of interventricular septum was significantly impaired in all Ang1CKO embryos compared with control at E13.5-E14.0 presumably due to the impaired myocardial growth (Fig. 3e,g, Supplementary Fig. 4a,b). Taken together, these findings indicate that the embryonic lethality of Agn1CKO embryos between E12.5 and E14.5 might be ascribed to the combinatorial defects in both coronary vein formation and myocardial growth.

Ang1 is predominantly expressed in the atria and ventricles. We next examined the expression pattern of Ang1 in the embryonic heart during coronary vessel formation. We generated an *Ang1-mCherry* reporter mouse as described in Methods, since commercial antibodies were not available to detect the endogenous expression of Ang1 in murine tissue. Immunostaining with an anti-DsRed antibody in the cryosectioned samples of Ang1-mCherry reporter mice demonstrated that Ang1 was strongly expressed in the atria and ventricles to a similar extent at E11.5 (Supplementary Fig. 5a). At E13.5, Ang1 expression was confined to the atria and ventricular trabeculae (Supplementary Fig. 5b).

We next evaluated the expression of Tie2 by X-gal staining using *Tie2-lacZ* transgenic mice[30]. At E10.5, the strongest Tie2-lacZ signal in the cardiovascular system of these mice was detected in the SV (Fig. 5a,b). Tie2-lacZ signals were also observed in the endocardial endothelium of the atria and ventricles at E10.5, but were markedly weaker than those in the SV (Fig. 5a,b), indicating that Ang1 may be involved in the migration of Tie2-positive ECs of the SV toward the myocardium.

Myocardial Ang1 attracts Tie2-positive ECs from SV. Previous study suggested that the ECs of the SV are one of the most plausible candidate sources of coronary ECs[9]. In addition, Tie2 was most strongly expressed in the ECs of the SV at E10.5, when the ECs of the SV begin to invade the atrium (Fig. 5a,b). Thus, we hypothesized that myocardial Ang1 might attract the ECs of the SV. Therefore, we examined whether myocardial Ang1 is indeed responsible for the migration of ECs from the SV into the ventricular myocardium by using a cardiac organ culture system modified to enable the detection of Tie2-lacZ-positive ECs migrating from the SV[9,30]. Developing hearts were isolated from *Tie2-lacZ* transgenic mice, *Ang1flox/flox* (control) mice or Ang1CKO mice at E10.5, after the proepicardium has spread over the heart surface to form the epicardium but before any coronary sprouts are present. Since Tie2-lacZ was expressed in the endocardial endothelium of the embryonic heart, Tie2-lacZ signals were detected throughout the embryonic heart when the intact hearts were resected from *Tie2-lacZ* transgenic mice, cultured for 72 h and stained with X-gal (Supplementary Fig. 6a). On the contrary, no Tie2-lacZ-positive signals were detected throughout the embryonic heart resected from wild-type (control) embryos (Supplementary Fig. 6b). Therefore, the hearts were dissected to separate the ventricles with their epicardial covering (V + Epi) from the SV and atria (SV + A). When the SV + A or V + Epi resected from Tie2-lacZ mice were cultured separately for 72 h and stained with X-gal,